

See discussions, stats, and author profiles for this publication at: <https://www.researchgate.net/publication/6176686>

Evidence of Wormlike Micellar Behavior in Chromonic Liquid Crystals: Rheological, X-ray, and Dielectric Studies

ARTICLE *in* THE JOURNAL OF PHYSICAL CHEMISTRY B · SEPTEMBER 2007

Impact Factor: 3.3 · DOI: 10.1021/jp073190+ · Source: PubMed

CITATIONS

29

READS

48

4 AUTHORS:



Kris Prasad

Centre for Nano and Soft Matter Sciences

295 PUBLICATIONS 2,961 CITATIONS

SEE PROFILE



Geetha Nair

Centre for Nano and Soft Matter Sciences

77 PUBLICATIONS 1,040 CITATIONS

SEE PROFILE



Gurumurthy Hegde

BMS R and D Centre

100 PUBLICATIONS 379 CITATIONS

SEE PROFILE



Jayalakshmi Vallamkonda

National Institute of Technology, Warangal

14 PUBLICATIONS 125 CITATIONS

SEE PROFILE

Evidence of Wormlike Micellar Behavior in Chromonic Liquid Crystals: Rheological, X-ray, and Dielectric Studies

S. Krishna Prasad,* Geetha G. Nair, Gurumurthy Hegde,[†] and V. Jayalakshmi

Centre for Liquid Crystal Research, Jalahalli, Bangalore 560013, India

Received: April 25, 2007; In Final Form: June 22, 2007

We report rheological, X-ray, and dielectric investigations on a chromonic liquid-crystalline system formed by aqueous solutions of a food coloring agent, Sunset Yellow, in the absence and upon addition of salt. The salt-concentration dependence of the steady-state viscosity at low shear rates has a non-monotonic variation and is qualitatively similar to the behavior seen in wormlike micellar systems, a surprising result since chromonic systems are expected to be non-micellar in character. More interestingly, for a particular low concentration of the salt (20 mM), the viscosity increases by 3 orders of magnitude in comparison with that of the pure chromonic material. The dynamic (oscillatory) rheological data bring out features which can be described in terms of a microstructure formation. X-ray and dielectric studies show that certain characters of the aggregates formed by the Sunset Yellow molecules are not altered by the addition of salt.

Introduction

Investigations on a novel class of lyotropic mesophases, referred to as chromonic liquid crystals (CLCs), have been attracting significant attention in recent years.^{1–7} Chromolyn, an anti-asthmatic drug, and perhaps the most extensively studied CLC, lends its name to this class of materials. The novelty of CLCs arises due to several contrasting features that they exhibit, namely, (i) structurally these molecules do not consist of the aliphatic chain, an essential ingredient in the conventional lyotropic LCs (amphiphilic mesogens such as soaps and biological lipids); (ii) assembly-wise they do not form micelles, which are the basic building blocks of lyotropic systems; and (iii) the associated aggregation of the molecules shows isodesmic behavior as opposed to the non-isodesmic behavior of lyotropics. The interest in CLCs is also due to their promising applications in antibiotics, anticancer agents, and as aligning agents/compensating plates in technologically important display devices. Apart from the medically important material mentioned above, certain dyes employed in the textile industry and a food coloring agent, Sunset Yellow FCF, have been investigated.^{7–9}

In CLCs, the ionic or hydroxyl groups are present around the periphery of the hydrophobic aromatic rings. In order to minimize the surface area in contact with the surrounding aqueous medium and more importantly owing to the π – π^* attraction between the aromatic parts, which to a large extent are planar, the molecules tend to form face-to-face stacking leading to the formation of columns. Compared to other CLCs, there have been only a few studies on Sunset Yellow FCF. While Luoma⁷ investigated optical, magnetic, and X-ray properties, birefringence and X-ray measurements were reported by Horowitz et al.⁹ When dissolved in water, Sunset Yellow FCF exhibits two mesophases depending on the concentration. At high concentrations of the dye, a hexagonal columnar structure termed M phase is seen in which the columns pack into a hexagonal

lattice quite similar to those in thermotropic discotic systems and exhibit both orientational and positional orders. At low concentrations, the columns still exist but the positional order is lost, leading to the appearance of the nematic (N) phase.

Here we report rheological, dielectric, and X-ray diffraction studies in the N phase of Sunset Yellow FCF and its mixtures with a salt, namely, sodium chloride. The results demonstrate that the addition of salt can significantly influence the properties of the chromonic system. The rheological behavior suggests the presence of microstructures. The dependence of the magnitude of the viscosity on the salt concentration mimics the behavior seen in the conventional lyotropic systems that exhibit wormlike micelles.¹⁰

Experimental

Materials. The chromonic dye Sunset Yellow FCF, whose chemical structure is shown in Figure 1, was purchased from Aldrich and was used without further purification. To get the liquid crystalline state, solutions of Sunset Yellow were made in D₂O (Aldrich). The mixtures were prepared by adding weighed amounts of Sunset Yellow to a known volume of D₂O, immediately capping the container, and vortexing the contents for 1 h, after which the solution appeared homogeneous. All the measurements to be described in this paper have been performed on 1 M aqueous solutions of Sunset Yellow, which we hereafter refer to as SSY. Pure (99.5%) sodium chloride was purchased from Ranbaxy Fine Chemicals and was used as is. In all the experiments, the time between the preparation of the mixture and the actual measurements was minimized, to the extent possible, to reduce any effect of concentration change. It is known² that the major difference in the phase behavior obtained by using D₂O instead of H₂O is that the transition lines are merely shifted upward by about 5 °C.

Methods. *Rheology.* Rheological measurements were performed on a controlled-stress rheometer (AR-G2, TA Instruments) equipped with a Peltier-based temperature control. A cone-and-plate geometry, with a cone diameter of 20 mm and cone angle of 2°, was employed. The solvent-trap of the

* Corresponding author. E-mail: skpras@gmail.com.

[†] Present address: Department of Electronics and Computer Engineering, Hong Kong University of Science and Technology, Clear Water Bay, Kowloon, Hong Kong.

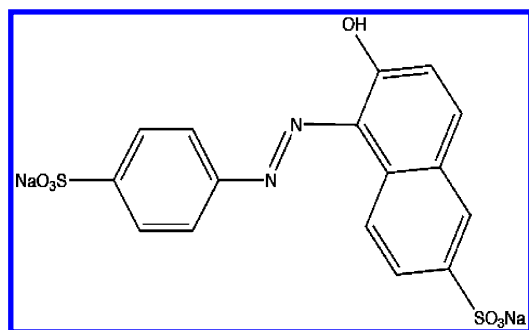


Figure 1. Chemical structure of the dye Sunset Yellow.

geometry was filled with D₂O to avoid evaporation of water and consequently a change of concentration during the experiments. All the rheological measurements have been done at a fixed temperature of 25 °C.

X-ray Diffraction. Small-angle X-ray scattering measurements were performed using an image plate setup described elsewhere¹¹ The samples were contained in Lindemann capillaries, and Cu K α radiation ($\lambda = 0.154$ nm), obtained with the help of two orthogonally mounted parabolic mirrors, was employed. After filling the sample in the high-humidity chamber, the two ends of the capillaries were sealed using an epoxy.

Dielectric Studies. For these studies the samples were contained between two ITO-coated glass plates with well-defined electrode areas. The typical sample thickness defined by PET spacers was in the range of 10 μ m. The cells sealed on all sides, except for two narrow openings, were kept in the high-humidity chamber and filled with the sample at room temperature by capillary action. After complete filling of the cell, the narrow openings were also sealed with the epoxy. The frequency-dependent dielectric spectrum was obtained using an Impedance/Gain Phase Analyzer (Solatron SI1260) in conjunction with a broadband dielectric converter (Novocontrol). Owing to the high conductivity of the samples investigated, even the oscillating probe voltage used in the standard measurements could lead to local heating. To minimize such effects, a low magnitude of the oscillating voltage (100 mV) was used to perform the measurements.

Results and Discussion

Phase Behavior. At 1 M concentration in aqueous solution, Sunset Yellow is expected to show the nematic phase at room temperature. Indeed, optical polarizing microscopy (OPM) observations reveal the schlieren brush texture characteristic of the N phase (see Figure 2 a). Mixtures with different salt concentrations (X_{salt}) studied here also exhibit the N phase at room temperature. The thread texture seen for a representative mixture ($X_{\text{salt}} = 50$ mM) shown in Figure 2b is also a typical texture of the N phase. Interestingly, the material sandwiched between a glass slide and a cover slip appeared to have much higher viscosity in the case of the $X_{\text{salt}} = 50$ mM mixture as compared to that for the SSY material, a feature that is corroborated in the rheological measurements described below.

Rheological Measurements. Steady-State Rheology. Figure 3 shows the dependence of viscosity η on the shear rate obtained at 25 °C for the SSY sample containing no salt. The behavior can be divided into three distinct regions: shear-rate-independent regions I and III, and the strongly shear-dependent region II. The observation of such Newtonian behavior followed by a shear-thinning region has been reported for another chromonic system also.² It should be pointed out that the extent to which the data in region I was independent of shear rate appeared to

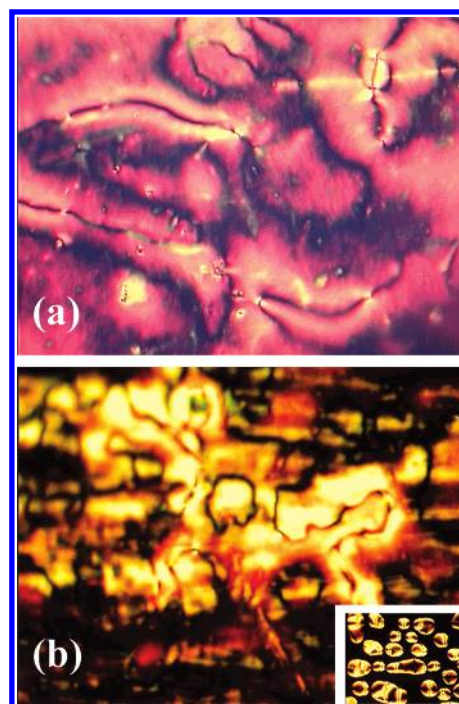


Figure 2. Photomicrographs of the pattern observed in the nematic phase between crossed polarizers: (a) schlieren texture seen for the SSY material, and (b) thread texture exhibited by SSY + 50 mM salt mixture. The inset shows the appearance of the nematic from the isotropic phase.

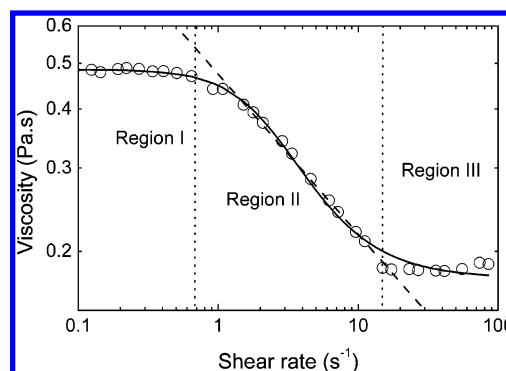


Figure 3. Shear-rate dependence of the viscosity for the SSY sample, exhibiting shear thinning. The solid line represents fitting the data over the entire range to the Carreau model (eq 1), and the dashed line corresponds to the power-law fitting to the data in the shear-thinning region II.

be dependent on the experimental conditions including sample loading (the maximum change in the magnitude of the value at the lowest shear rate used, varied in the range 0.25–0.8 between different experiments). However, the behavior seen in regions II and III was always reproducible. The interesting feature is the shear thinning observed in SSY, a feature common in polymeric systems. It must be remarked, however, that the degree of shear thinning in the present case is quite modest with η decreasing by only a factor of 2, whereas in polymer melts η falls by orders of magnitude as the shear rate increases.¹² Considering the fact that it was observed² in the case of the nematic phase of cromolyn dye also, we suggest that the shear-thinning behavior could be characteristic of the chromonic systems.

The shear-rate dependence of η through all the regions could be described by the four-parameter constitutive function referred to as the Carreau model:¹³

$$\eta(\dot{\gamma}) = \eta_{\infty} + \frac{\eta_0 - \eta_{\infty}}{\left(1 + \left(\frac{\dot{\gamma}}{\dot{\gamma}_0}\right)^2\right)^{(1-n)/2}} \quad (1)$$

where $\dot{\gamma}_0$ represents the shear-rate value below which the viscosity approaches the (low shear rate) limiting value η_0 and the material behaves as a Newtonian fluid, η_{∞} is the limiting value of the second Newtonian plateau at high shear rates, and n is the important power-law index. The solid line through the data in Figure 3 shows that the Carreau equation describes the data well in regions I and II, but less satisfactorily in region III, with the exponent $n = 0.35 \pm 0.06$. (Fitting the data to the more generalized expression, known as the Carreau–Yasuda equation¹⁴ wherein the numeral 2 in eq 1 is replaced by a variable, did not yield significantly better results). It is interesting to note that the value of $n = 0.35$ is in the range obtained for shear-thinning polymers.¹⁵ In the shear-thinning region, considering that $\eta \ll \eta_0$ and $\eta \gg \eta_{\infty}$, it is customary to describe the data with a power law in the shear rate, $\eta = K\dot{\gamma}^m$. Here, K is a prefactor giving the value of η when $\dot{\gamma} = 1/\text{s}$. For a Newtonian fluid $m = 0$. Fitting the data in region II we get the exponent to be -0.34 ± 0.01 , in conformity with the value obtained through eq 1. We now turn our attention to the influence of the NaCl concentration (X_{salt}) on the steady-state rheological behavior. Figure 4 shows the data for mixtures with various salt concentrations obtained at 25 °C. For comparison, the data for the no-salt SSY material is also shown. Notice the huge changes in the viscosity values for the different mixtures. What is more surprising is that even on a qualitative level it is seen that the magnitude of the viscosity at low shear rates does not change monotonically with X_{salt} . In each case a shear-thinning effect is seen, although except for $X_{\text{salt}} = 310$ mM mixture, a plateau was not observed at low shear rates. However, all the mixtures studied exhibit the second plateau region in which the viscosity is very weakly dependent on the shear rate. Also seen was that except for the SSY material and the $X_{\text{salt}} = 310$ mM mixture, the shear thinning occurred over a range of shear-rate values. Some of these features are seen in other soft condensed matter.¹² A feature that is prominent for $X_{\text{salt}} = 20$ mM mixture and to a lesser extent in other mixtures is the appearance of oscillations at the crossover point between the shear-thinning region and the high-shear-rate plateau region. To our knowledge such a behavior has not been observed either in polymeric or in lyotropic systems. (It should be emphasized that this feature is highly reproducible). A parameter that can be taken to be a measure of the influence of the salt concentration on the magnitude of viscosity is its value at zero shear rate. As mentioned above, some of the mixtures studied here do not show a clear saturation in the viscosity value at low shear rates. Therefore, we show in Figure 5 η_{low} the value determined at a low-shear-rate value of $3 \times 10^{-3}/\text{s}$. We observe a drastic increase in η_{low} by 3 orders of magnitude for the lowest salt concentration (20 mM) mixture, a decrease for the next higher concentration (50 mM), followed by a broad maximum for further increase in X_{salt} . (It may be noted that an earlier work² has reported a monotonic increase in viscosity as a function of the salt concentration. This could be perhaps because lower salt concentrations were not investigated.) This behavior mimics the features observed in aqueous micellar solutions formed by surfactants like CTAB doped with salt acting as counterions^{10,16} having wormlike micelles and analyzed in terms of a reptation model. In such systems, cylindrical micelles can grow into very long wormlike micelles with increasing surfactant concentration. Because of their long flexible structure, they entangle and form

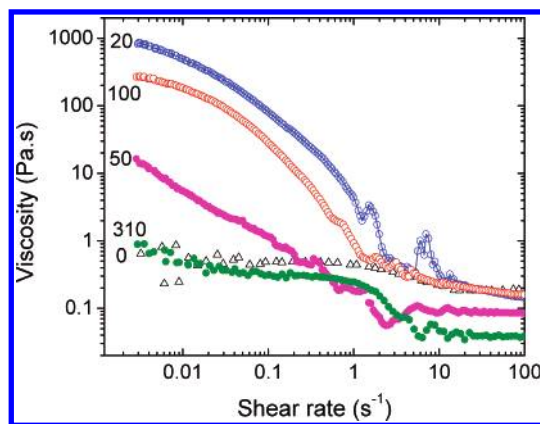


Figure 4. Influence of salt concentration on the steady-state viscosity for a fixed value of Sunset Yellow in the mixture. The number next to each data set indicates the salt concentration in the mixture. All the materials exhibit shear-thinning behavior, while the Newtonian type of behavior at low shear rates is not obvious in the case of $X_{\text{salt}} = 50$ mM mixture. To be noted is the non-monotonic variation in the magnitude of the low-shear-rate viscosity as a function of the salt concentration. (The data for SSY, shown as open triangles, are given for comparison).

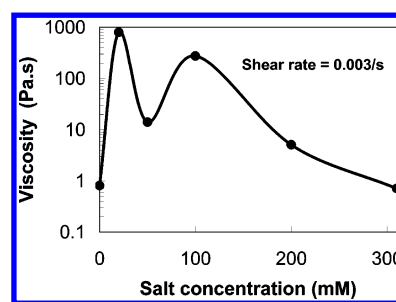


Figure 5. Salt-concentration dependence of the apparent viscosity at very low shear rate (0.003 s^{-1}) showing the 3 orders of magnitude increase in the value between the 20 mM mixture and the SSY material without salt. The profile of the non-monotonic variation seen is qualitatively similar to the behavior in lyotropic systems exhibiting wormlike micelles.

complex networks. Since these micelles are only held together by relatively weak physical attractions/repulsions, they can easily form and break, the dynamics of which can be controlled by the concentration of the salt.¹⁷ The similarity between the lyotropic systems and the chromonic system under study is somewhat surprising, since the latter is not expected to form any micellar structure. It may, however, be remarked that the theoretical work of Maiti et al.⁴ indeed suggested that in chromonic systems short columns aggregate to form chainlike or wormlike aggregates owing to stronger excluded volume interactions.

Dynamic Measurements. We first determined the linear viscoelastic regime (LVR) for the SSY sample by performing oscillatory measurements sweeping the strain amplitude γ from 10^{-2} to 1, at a fixed angular frequency $\omega = 1 \text{ rad s}^{-1}$. As seen in Figure 6a, for the freshly mounted sample, both the storage (G') and loss (G'') moduli are independent of the strain amplitude over the entire range of measurement. More importantly, it may be noticed that $G' > G''$ by more than order of magnitude over the entire range. In contrast, when measurements are done after a strong preshear is applied to the sample for 600 s at a shear rate of 50/s, G' decreases by an order of magnitude but G'' increases slightly and remains more than G' for all values of strain amplitude (see Figure 6b). It is also seen that the LVR region is slightly reduced for G'' after the preshear treatment.

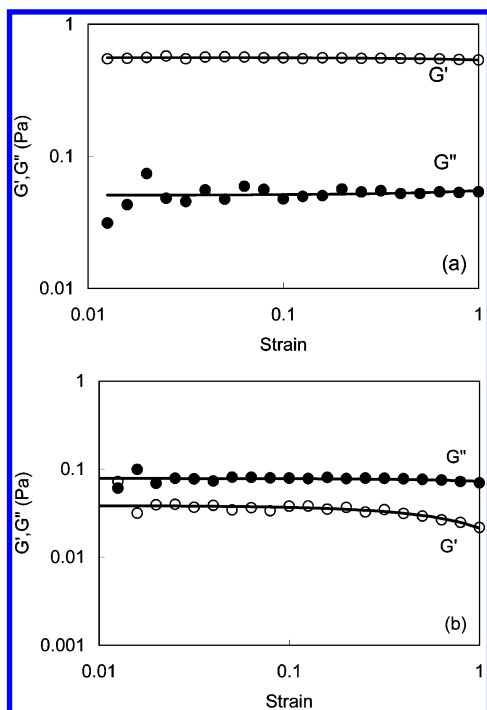


Figure 6. Dependence of the storage (G' : \circ) and loss (G'' : \bullet) moduli as a function of the applied strain for the SSY material (a) before and (b) after a preshear treatment for 600 s at a shear rate of 50 s^{-1} . Notice that the freshly mounted sample (before preshear treatment) has a solidlike behavior ($G' > G''$) and has the linear viscoelastic regime (LVR) over the entire range of strain studied. After application of preshear, the system behaves like a liquid ($G'' > G'$). These features suggest the presence of microstructures in the medium.

Angular frequency-dependent oscillatory experiments were carried out at fixed strain amplitude well within the LVR region. The viscoelasticity data thus determined for the SSY sample before and after the preshear treatment mentioned above are given in Figure 7, parts a and b. In the freshly mounted sample, at low frequencies the elastic part

dominates and is weakly dependent on the frequency. In contrast, the viscous part (loss modulus) varies linearly in the log-log space with a crossover (from $G' > G''$ to $G'' > G'$ behavior) at $\sim 10 \text{ rad s}^{-1}$. In other words, the sample behaves solidlike over most of the frequency range. On the other hand, the presheared sample behaves like a liquid with $G'' > G'$ throughout the frequency range. For a fluid with Maxwellian behavior, the following relations are valid when the applied angular frequency ω is smaller than the inverse of the relaxation time τ (i.e., when $\omega\tau \ll 1$):

$$G'(\omega) = \eta\tau\omega^2 \quad (2)$$

$$G''(\omega) = \eta\omega \quad (3)$$

where η is an effective viscosity. According to these relations, the slope of the G'' versus ω curve should have a slope of 1, and the G' versus ω curve should have a slope of 2. But what is experimentally observed is that G'' has the expected behavior while the slope for the G' curve is only 1.2 ± 0.02 . (Since there is a slowing down of the G' data below 10 rad s^{-1} , a feature not seen in the G'' set, we fit the data that lies above this frequency).

Frequency dependence of G' and G'' before and after preshear treatment are shown for one salt mixture ($X_{\text{salt}} = 20 \text{ mM}$) in Figure 8, parts a and b. At low frequencies, unlike the SSY material, the mixture has $G'' > G'$, although the difference

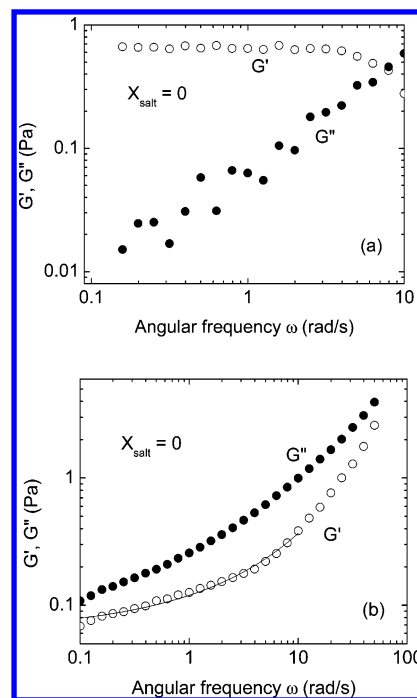


Figure 7. Angular frequency dependence of the moduli for the SSY sample (a) before and (b) after the preshear treatment. The storage modulus seems to be nearly independent of frequency, especially at lower frequencies, and remains higher than the loss modulus over most of the ω range. The preshear treatment causes the storage modulus to decrease substantially and to be lower than the loss modulus over the entire range. For $\omega > 10 \text{ rad s}^{-1}$, the slope of the G'' variation is 1.0, expected for a Maxwellian fluid, whereas for G' it is 1.2. Notice that G' appears to have a terminal behavior at low frequencies, as suggested by the line drawn through the data points.

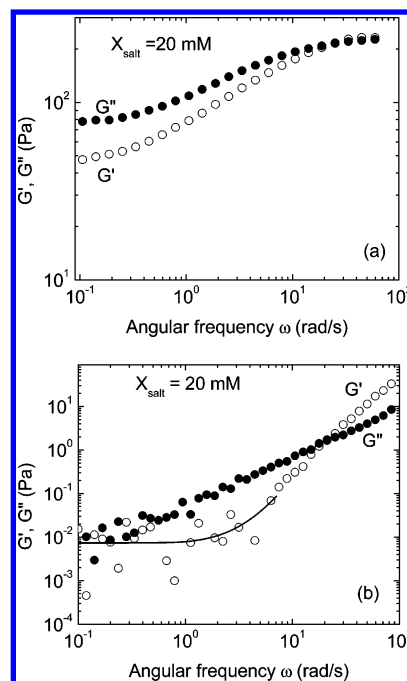


Figure 8. Variation of G' and G'' with angular frequency for $X_{\text{salt}} = 20 \text{ mM}$ mixture (a) before and (b) after the preshear treatment. Although the absolute values of both moduli come down upon preshear, in the low-frequency region, the relation $G'' > G'$ remains. The terminal behavior of G' is suggested by drawing a line through the data at low frequencies.

between the two parameters is small. Further, after preshear treatment the storage modulus has a “terminal” behavior for both materials, that is, G' reaches a limiting value G'_0 , at low

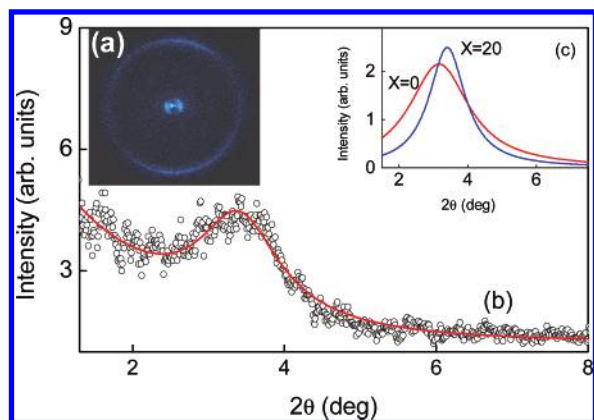


Figure 9. (a) X-ray diffraction pattern in the N phase and (b) its radial intensity profile at low angles. The sharp wide-angle arc in (a) arises from the spacing between two molecules within the same aggregate, whereas the diffuse scattering in (a) and the peak in (b) correspond to the diffraction from the aggregate dimension. The line through the data in (b) represents the fit to a Lorentzian expression with a background term. (c) The low-angle profiles for the SSY ($X = 0$, red curve) and the 20 mM salt mixture ($X = 20$, blue curve) with background subtraction. Notice that the Bragg angle is increased and the peak is narrowed slightly for the mixture.

frequencies, as suggested by the lines drawn in Figures 7b and 8b. The G'_0 value for the mixture is about an order of magnitude lower, although before preshear it is 70 times higher. Another difference between the SSY material and the mixture is that the slopes of G' and G'' are 2.1 ± 0.01 and 1.1 ± 0.01 , respectively, and are thus very close to the expectations from eqs 2 and 3.

X-ray Diffraction Measurements. We carried out X-ray diffraction measurements on SSY as well as a representative mixture with salt, namely, $X_{\text{salt}} = 20$ mM, to find out if there are any structural changes upon addition of salt. Figure 9a shows the diffraction pattern obtained in the N phase of the mixture. The pattern showing evidence of flow alignment of the director has a broad diffuse scattering at low angles along the equatorial direction and a sharp arc at wide angles along the meridional direction. Azimuthal angle scans taken indicate that the two reflections are at 90° with respect to each other. A similar pattern was obtained for the SSY sample and is in agreement with the results for the N phase of chromonic systems reported by Horowitz et al.⁹ for the Sunset Yellow/H₂O system and Goldfarb et al.¹⁸ for DSCG. The wide-angle reflection corresponds to a spacing of 0.334 nm in both SSY and the mixture. The N phase in chromonic systems has been described to consist of stacks of chromonic molecules in a columnar fashion with the intercolumnar interaction being restricted to only orientational order^{9,18} (similar to the N_{col} phase in thermotropic systems¹⁹). The 0.334 nm spacing observed thus corresponds to the distance between the molecules arranged in a cofacial manner within the columnar stacks. Figure 9b gives the radial intensity profile in the low-angle region of the pattern shown in Figure 9a. The fact that the peak observed is broad and diffuse confirms the nematic character of the phase. To extract the peak parameters, the data was fitted to a Lorentzian expression with an exponential background term. To emphasize the influence of the addition of salt, the fitted profiles for SSY and the mixture are shown in Figure 9c. Evidently, the peak position shifts to higher scattering angles and the profile is slightly sharper for the mixture. The spacing corresponding to the peak position (approximate distance between the stacks) decreases from 3.0 nm for SSY to 2.83 nm for the mixture. The half width at half-maximum (HWHM), which is inversely proportional to the

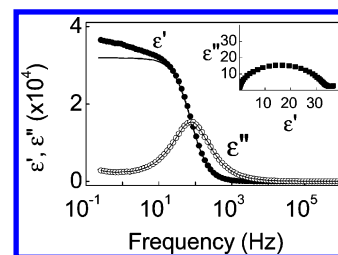


Figure 10. Frequency spectra of the real (ϵ' : ●) and the imaginary (ϵ'' : ○) parts of the dielectric constant for the SSY sample. Fitting the data to the Havriliak–Negami equation (eq 4), shown as a line, yields a relaxation frequency of 74 Hz, as is indeed suggested by the peak in ϵ'' . The inset shows the Argand diagram of ϵ' vs ϵ'' depicting a Cole–Cole arc (both the axes have been scaled down by a factor of 1000 for convenience).

distance over which the motion of the different columnar stacks is correlated, decreases upon addition of salt. The correlation length calculated from the HWHM of the peak profiles increases from 8 nm for SSY to 12 nm for the mixture. The value of 8 nm for SSY again agrees with that reported by Horowitz et al.⁹ for Sunset Yellow.

Dielectric Measurements. Figure 10 shows the frequency spectrum of the real (ϵ') and imaginary (ϵ'') parts of the dielectric constant for SSY. Notice that there is a sharp drop in ϵ' and a peak in ϵ'' around 70 Hz indicating a clear relaxation mode. To extract the relaxation parameters (frequency f_R and dielectric strength ϵ_R) the data were fit to the Havriliak–Negami (HN) equation:²⁰ where f is the measuring frequency, ϵ_∞ is the sum

$$\epsilon^*(f) = i\sigma(f) + \epsilon_\infty + \frac{\epsilon_R}{[1 + (if/f_R)^\alpha]^\beta} \quad (4)$$

of the dielectric strengths of all the high-frequency modes other than the one under consideration, ϵ_R is the difference between low- and high-frequency dielectric constants and is a measure of the dielectric strength of the mode of interest, and f_R is the characteristic relaxation frequency. The parameters α and β describe the width and asymmetric broadening of the relaxation curve; $\alpha = 1$ and $\beta = 1$ stand for a Debye curve. To account for the DC conductivity (σ) contribution to the imaginary part of the dielectric constant, the term $i\sigma(f)$ was needed. Notice that the ϵ' data also show a slow increase with decreasing frequency in the low-frequency region. This should be due to the electric double layer formation. We do not take this into account here since the interest is only about the relaxation mode occurring at ~ 70 Hz. Figure 10 also shows the fitting done to eq 4. The extracted values of α and β are 0.95 ± 0.005 and 1 ± 0.005 , respectively, indicating that the mode has the characteristics of a Debye mode as is graphically seen in the Argand diagram shown in the inset of Figure 10. The fitted values of the relaxation frequency f_R and the strength of the mode ϵ_R are 74.4 ± 0.4 Hz and 31920 ± 320 , respectively. The large value of ϵ_R is caused by the OH group and is typical of hydrogen-bonded systems.²¹ We attribute the relaxation as a director mode associated with the fluctuations of the stacks about their short axis. The presence of the hydrogen bond as well as the formation of the aggregates results in the relaxation frequency being quite low. Similar features were seen for the $X_{\text{salt}} = 20$ mM mixture, except that the value of the relaxation frequency doubles to $f_R = 162$ Hz (see Figure 11).

Finally, we comment on the cause for the rheological behavior in the light of the X-ray and dielectric data. The fact that the low-shear-rate viscosity η_{low} is already high for the two chromonic systems (even in the absence of salt) which have

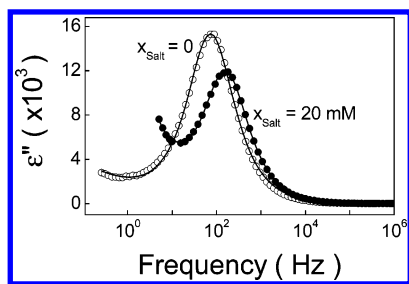


Figure 11. Comparative dielectric absorption spectra for SSY (○) and the 20 mM mixture (●). Both the data sets have a near-Debye behavior, with the relaxation frequency being slightly higher for the mixture.

been studied—Sunset Yellow in the present case and DSCG by Kostko et al.²—can be attributed to the hydrogen-bond formation. The situation perhaps then would be quite similar to the fragile network observed in the case of liquid-crystalline material embedded in aerosil matrices.²¹ The solidlike dynamic viscoelastic parameters shown in Figure 6 support such a possibility. The X-ray and dielectric data show that neither the dimension of the aggregates nor the dynamics associated with them alter significantly with the addition of salt. Thus, the primary influence of the salt would be on the microstructure due to the hydrogen bonding of the system and not on the individual aggregates.

In summary, we have performed rheological, X-ray, and dielectric investigations on a chromonic liquid-crystalline system formed by a food coloring agent, Sunset Yellow, in the absence and upon addition of salt. Steady-state viscosity measurements show non-monotonic change in the viscosity value as the salt concentration is changed and, for a particular concentration, reach a value that is as high as 3 orders of magnitude compared to that without salt. The salt-concentration dependence of the viscosity is similar to that seen in region I systems forming a wormlike micellar structure. The oscillatory measurements bring out features which can be described in terms of a microstructure formation. X-ray and dielectric studies show that certain characters of the aggregates formed by the Sunset Yellow molecules are not altered by the addition of salt.

Acknowledgment. The authors express their sincere thanks to Dr. D. S. Shankar Rao for his help in the X-ray experiments.

Thanks are also due to Mr. Chethan V. Lobo for his assistance during the setting up of the rheometer.

References and Notes

- (1) Lydon, J. *Curr. Opin. Colloid Interface Sci.* **2004**, *8*, 480, and references therein.
- (2) Kostko, A. F.; Cipriano, B. H.; Pinchuk, O.; Ziserman, L.; Anisimov, M. A.; Danino, D.; Raghavan, S. R. *J. Phys. Chem. B* **2005**, *109*, 19126.
- (3) Nastishin, Y. A.; Liu, H.; Schneider, T.; Nazarenko, V.; Vasyuta, R.; Shiyanovskii, S. V.; Lavrentovich, O. D. *Phys. Rev. E* **2005**, *72*, 041711.
- (4) Maiti, P. K.; Lansac, Y.; Glaser, M. A.; Clark, N. A. *Liq. Cryst.* **2002**, *29*, 619.1.
- (5) Schnieder, T.; Lavrentovich, O. D. *Langmuir* **2000**, *16*, 5227.
- (6) Harrison, W. J.; Mateer, D. L.; Tiddy, G. J. *J. Phys. Chem.* **1996**, *100*, 2310.
- (7) Luoma, R. J. Ph.D. Thesis, Brandeis University, Waltham, MA, 1995.
- (8) Horowitz, V. R. Thesis, University of Pennsylvania, Philadelphia, PA, 2005; <http://www.sccs.swarthmore.edu/users/05/viva/SunsetYellow/Thesis/Thesis.pdf>.
- (9) Horowitz, V. R.; Janowitz, L. A.; Modic, A. L.; Heiney, P. A.; Collings, P. J. *Phys. Rev. E* **2005**, *72*, 041710.
- (10) Hartmann, V.; Cressley, R. *Colloid Polym. Sci.* **1998**, *276*, 169.
- (11) Sandhya, K. L.; Prasad, S. K.; Rao, D. S. S.; Bahr, Ch. *Phys. Rev. E* **2002**, *66*, 031710.
- (12) See, for example, Larson, R. G. *The Structure and Rheology of Complex Fluids*; Oxford University Press: Oxford, 1999.
- (13) Carreau, P. J. *Trans. Soc. Rheol.* **1972**, *16*, 99.
- (14) Yasuda, K.; Armstrong, R. C.; Cohen, R. E. *Rheol. Acta* **1981**, *20*, 163.
- (15) See, for example, Barnes, H. A.; Hutton, J. F.; Walters, K. *An Introduction to Rheology*; Elsevier: Amsterdam, 2005; Chan, C.; Gao, P. *Polymer* **2005**, *46*, 8151.
- (16) Rehage, H.; Hoffmann, H. *J. Phys. Chem.* **1988**, *92*, 4712.
- (17) Berret, J. In *Molecular Gels: Materials with Self-Assembled Fibrillar Networks*; Weiss, R. G., Terech, P., Eds.; Springer: The Netherlands, 2006; Chapter 19.
- (18) Goldfarb, D.; Luz, Z.; Spielberg, N.; Zimmermann, H. *Mol. Cryst. Liq. Cryst.* **1985**, *126*, 225.
- (19) Ringsdorf, H.; Wustefeld, R.; Zerta, E.; Ebert, M.; Wendorff, J. H. *Angew. Chem., Int. Ed. Engl.* **1989**, *28*, 914.
- (20) Havriliak, S.; Negami, S. *J. Polym. Sci. C* **1966**, *14*, 99.
- (21) Rao, D. S. S.; Prasad, S. K.; Prasad, V.; Kumar, S. *Phys. Rev. E* **1999**, *59*, 5572.
- (22) For a recent review, see Iannacchione, G. S. *Fluid Phase Equilib.* **2004**, *222–223*, 177.